

Numerical Approach of the Littoral Instability of Chalk Cliffs: Case of Grandes Dalles (The Large Flagstones)

M.C. Bedjaoui¹⁾, M.A. Allal¹⁾, A. Duperret²⁾, S. Taibi²⁾ and E. Rivoalen²⁾

¹⁾ Laboratory of EOLE, University of A.BELKAID, Tlemcen, Algeria, Chetouane BP 230, 13000 Tlemcen, m_bedjaoui@mail.univ-tlemcen.dz

²⁾ Laboratory of LOM, University of Havre, France, 53 Rue Prony, BP 540, 76058 Le Havre Cedex

ABSTRACT

The various situations representing coastal cliffs of Haute Normandy are tested on numerical models. The parameters taken into account are: the lithology of chalks and the presence or absence of fractures. It is a question of specifying the mechanical characteristics of chalk and the inside of the fractures. The chalk cliff of 80m height, with a vertical cliff face, is modeled in distinct elements in UDEC code. We consider initially the cliff with two layers, in dry and then in saturated state. Then, the cliff is taken with two layers; the chalk of Seaford constitutes the upper layer and the chalk of Lewes constitutes the lower layer, by introducing a fracture with a strong slope passing in the foot of the cliff and another time a fracture parallel with the cliff face.

KEYWORDS: Cliff, Chalk, Lithology, Fracture, UDEC code.

INTRODUCTION

The chalk cliffs of Haute Normandy are located on the French side of the Manche and undergo in the long term a high level of erosion of about 0.25 m/year (Costa, 2000; Dombusch and Al, 2001). Thus, following an observation period of several years, the erosion of chalk cliffs occurs by sudden collapses in Haute Normandy, Picardy (Dupperet et al., 2002, 2004) and in the northern region (Lahousse and Pierre, 2003). It is clear that the cliffs collapse under the combined action of several factors; climatic and oceanographic.

During the European research project ROCC (Risk Of Cliff Collapse), the geological investigation of the littoral was carried out (chalk lithology and recording fractures) as well as the determination of external agent

of terrestrial and marine origin contributing to the instability of chalk cliffs (for example, Mortimore et al., 2004). The knowledge of these parameters is necessary to approach the mechanical side of the phenomenon and to model the behavior of unstable cliffs.

In the present work, the factors to be considered are of a geological nature (lithology, fracture) and hydric (presence of water). Various situations are tested using numerical models. These are, essentially, the number of layers to be considered in the cliff, the mechanical characteristics of dry or saturated chalk and of the fractures having different dip.

NUMERICAL MODELING AND USED COMPUTER CODE

Numerical Formulation in UDEC

The UDEC computer code (Cundall, 1971; Itasca, 1999) uses a step by step procedure, called explicit

procedure. The equations of motion are solved to deduce new velocities and displacements starting from forces and stresses. Velocities and displacements are calculated starting from an equation of centered difference. Velocities are then employed to calculate the

rates of stresses, from which new stresses can be found by the constitutive equations. These calculations are carried out for one step of time, during which it is supposed that velocities are constant (see Fig. 1).

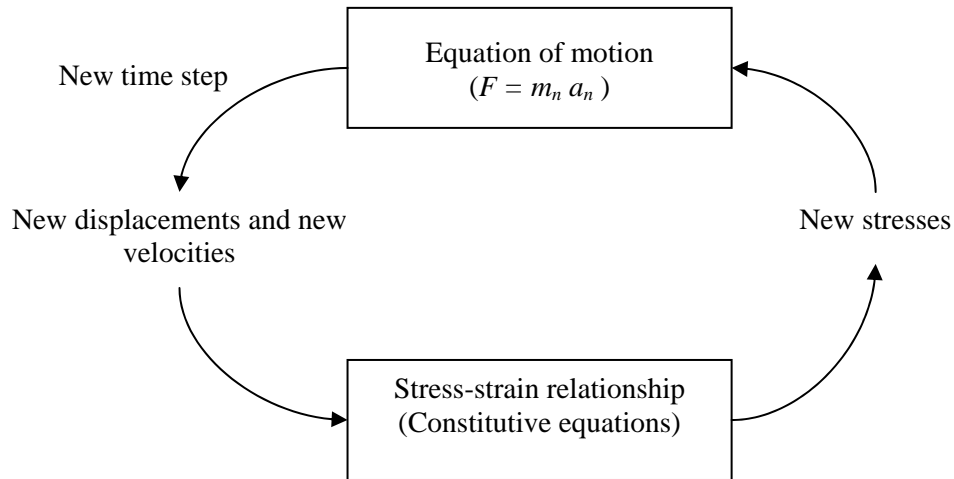


Figure (1): Cyclic calculation for the explicit methods in UDEC (Itasca, 1999)

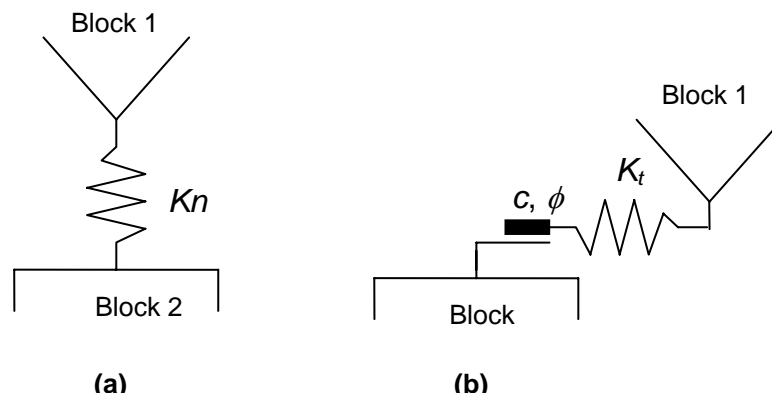


Figure (2): Modeling of the interaction between two blocks (Itasca, 1999)

Modeling

The medium is modeled by a finite number of blocks, separated by discontinuities crossing the solid

mass. If the deformation of the blocks is neglected in front of those of the crack, the solid mass is then a stacking of rigid blocks where all displacements

concentrate in the interfaces, blocks being subjected only to rigid body motion. Conversely, if the blocks are deformable, they are then discretized in triangular elements by finite differences, in which the deformation is constant.

The interaction between two blocks is modeled by a spring in the normal direction to the crack (Fig. 2a) and by a spring in series with a shoe in the direction of the crack (Fig. 2b).

Within each step of time, the increments of the normal stresses $\Delta\sigma_n$ and tangential stresses $\Delta\sigma_t$ acting on the crack are given by the following relations:

$$\Delta\sigma_n = K_n \Delta U_n \quad \text{and} \quad \Delta\sigma_t = K_t \Delta U_t \quad [1]$$

where ΔU_n and ΔU_t represent the increments of relative displacements in the normal and tangential direction to the crack, respectively. K_n and K_t represent the coefficients of normal and tangential stiffness.

The stress vector $(\sigma_n + \Delta\sigma_n, \sigma_t + \Delta\sigma_t)$ is to be projected on the strength criterion of the joint. This criterion is Mohr-Coulomb, defined by the cohesion c and the natural angle of friction ϕ .

Constitutive Models and Input Parameters

The UDEC code allows a large number of constitutive models to be used. In our study, the elastic-full-plastic constitutive model of Mohr-Coulomb is used for the intact rock and the criterion of Coulomb for the discontinuity.

As its name indicates, the constitutive model of Mohr-Coulomb is based on the failure criterion of Mohr-Coulomb, written as:

$$\tau_s = c + \sigma_n \tan \phi \quad [2]$$

or

$$\sigma_1 = \sigma_c + \frac{1 + \sin \phi}{1 - \sin \phi} \sigma_3 \quad [3]$$

The numerical execution of Mohr-Coulomb model in UDEC is as follows. Initially, an elastic phase for the increment of stress is calculated by using Hook's law. If all the stresses exceed the failure criterion, the stresses are corrected by using the flow rule and they are

reported again to the failure surface. A positive scalar is evaluated in this process, thereby determining the increment of plastic deformation. All this is done during one step of time, and the whole process is then repeated for the next time step.

The material properties which must be specified by using Mohr-Coulomb model are: the density ρ , Young modulus E , Poisson's ratio ν , the cohesion c , the angle of friction ϕ , the angle of dilatancy Ψ and the tensile strength σ_t .

By using the Coulomb criterion as constitutive model for the cracks, the failure occurs if the shear stress acting along the plan of the crack reaches the shear strength defined by Equations [2] and [3]. The input parameters for this model are: the cohesion c_j , the angle of friction ϕ_j and the tensile strength σ_{tj} of the crack.

Moreover, it is estimated that the elastic deformation of the crack follows a linear relation for the normal and tangential deformations. The input parameters for this are: the normal stiffness K_n and the tangential stiffness K_s . By using this constitutive model in UDEC, the deformation can occur at the level of the crack in the normal and tangential directions.

GENERAL CONSIDERATIONS

Geometry and Lithology of the Cliff

The study site is located in Haute Normandy (Fig.3), the part of Tilleul to Ault consists of chalk cliffs which are subject to instability. On the geological cross-section, we see that the zone is composed of different chalk. The part constituting the place known as Grandes Dalles (the Large Flagstones) is constituted of Upper Cretaceous chalk, where two lithologies outcrop: at the top chalk of Seaford and the base chalk of Lewes.

Fig. 4 represents the simplified geometry and the lithology of the perpendicular cross-section to the front of chalk cliff illustrating *in situ* the case of Grandes Dalles. The cliff is 80 m high. Lewes layer lies below the flat to a height of 50m and Seaford layer is just above it with a thickness of 30m.

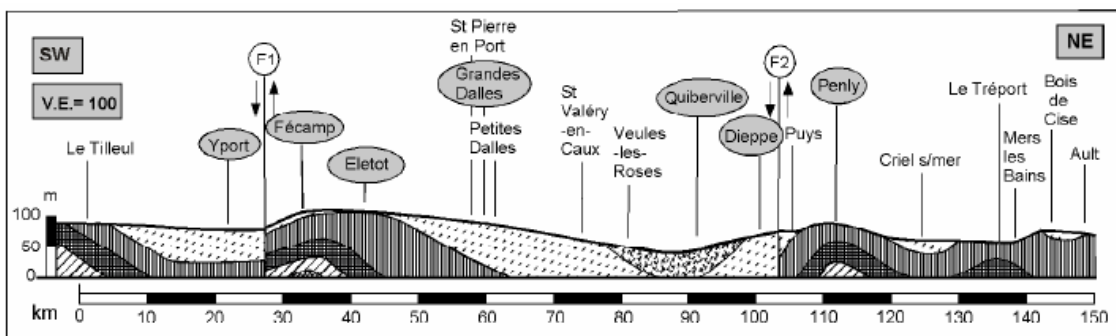
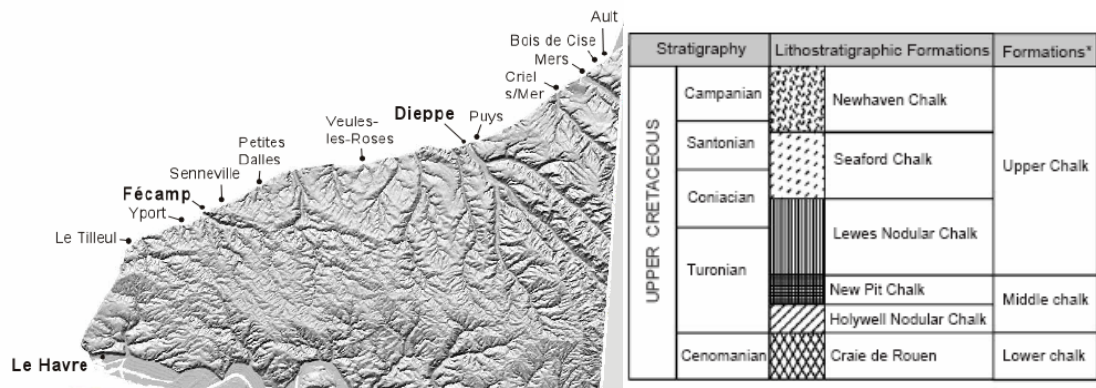


Figure (3): Geological cross-section of chalk coastal cliffs of the Haute Normandy and Picardie, France, with detail of the lithostratigraphic formation of chalk (Duperret et al., 2005)

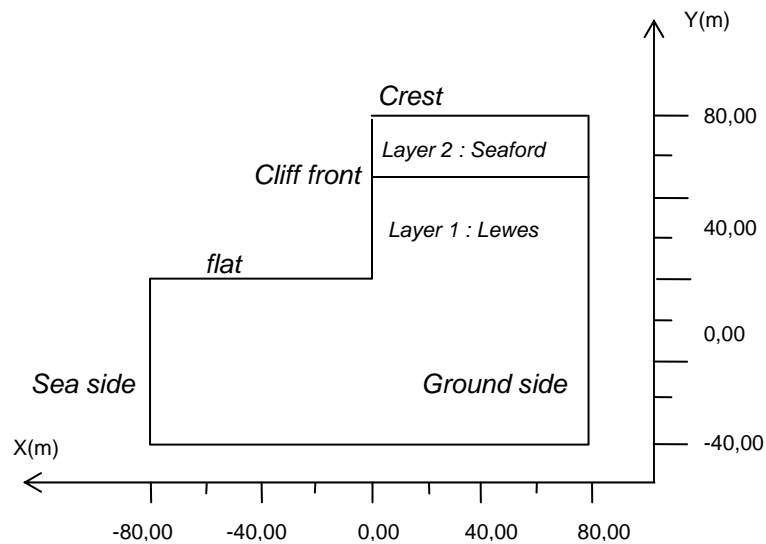


Figure (4): Perpendicular cross-section to the cliff front

Table (1): Mechanical characteristics of Lewes and Seaford (Ferhah, 2002; Duperret et al., 2005; Itasca, 1999)

Layer State	Lewes		Seaford	
	dry	saturated	dry	saturated
density, μ [Mg/m ³]	1.446	1.880	1.423	1.850
Young modulus, E [GPa]	0.600	0.250	0.400	0.187
Poisson's ratio, ν	0.3	0.3	0.3	0.3
angle of friction, ϕ [°]	33	15	30	19
cohesion, c [MPa]	1.1	0.8	0.95	0.4
tensile strength, σ_t [MPa]	0	0	0	0
angle of dilatancy, ψ^* [°]	10	10	10	10

* The angle of dilatancy is estimated starting from a range of data for various materials.

Table (2): Properties of the joint (Ferhah, 2002; Itasca, 1999; Indraratna, 2000; Farmhouse Ivars, 2006)

Properties	values
residual opening under high stress, (ares) [m]	0.0002
opening for a null normal stress, (azero) [m]	0.0005
cohesion, (jcohesion) [MPa]	0
angle of dilatancy [°]	0
angle of friction, (jfriction): [°]	27
normal stiffness, (jkn) [MPa/m]	1e11
tangential stiffness, (jks) [MPa/m]	1e10
permeability, (jperm) [m/j]	3.02e-2
tensile strength, (jtension) [MPa]	0

Boundary Conditions and Mechanical Characteristics

In addition, geometrical and kinematic boundary conditions indicated in the previous figure are imposed on the numerical models as follows:

- The lower limit of the modeled cliff has a null vertical displacement,
- The two side edges have a null horizontal displacement,
- The flat side, cliff front and the crest are free to any displacement.

Moreover, in the case of saturated cliff we consider a static groundwater. The hydraulic boundary conditions of the modeled cliff are:

- Impermeable lower edge,
- Triangular distribution of the hydrostatic pressure - ground side- (static groundwater supposed to reach the crest of the cliff).

The mechanical characteristics of chalk and the properties of the joint introduced into the model are given in Tables (1) and (2).

Some Mesh Dispositions

In UDEC, the deformable blocks are discretized in triangular elements of finite difference. The deformation of the blocks depends on the number of elements into which the blocks are divided (Itasca, 1999).

To study the effect of mesh on our structure, five sizes of mesh are selected: 2m, 4m, 6m, 8m and 10m. A horizontal fictitious joint in the foot of the cliff is introduced to have a uniform distribution of the mesh (see Figure 5).

For each size of mesh, a profile of stress and displacements is plotted in terms of the height of the cliff, once along cliff front and once at 13m inside the

solid mass. In UDEC, the displacements are calculated at the nodes while the stresses are calculated at the

center of the triangular element.

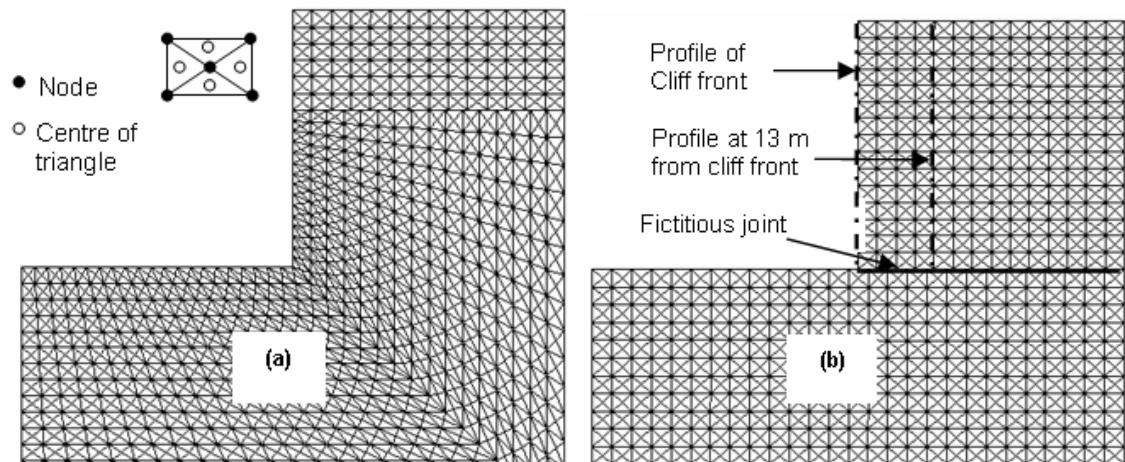


Figure (5): Grid in triangular elements: (A) joint fictionless, (b) with fictitious joint

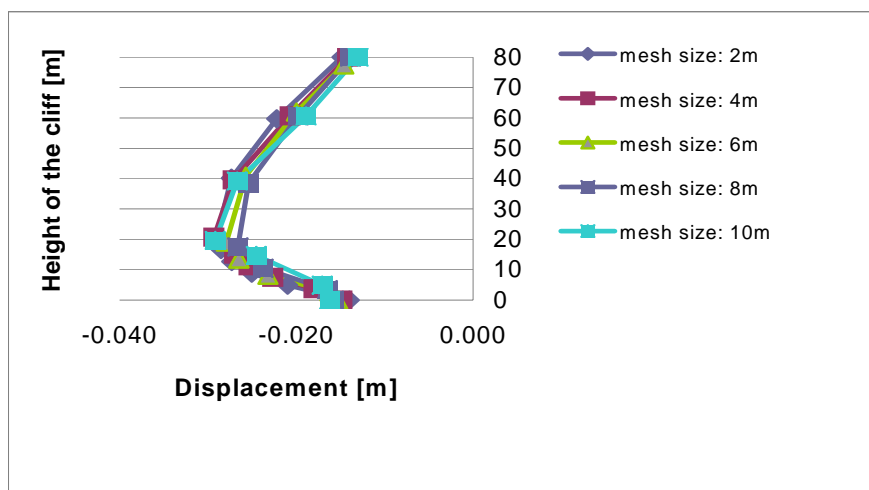


Figure (6): Horizontal displacement at the cliff front in terms of cliff height

Profile of Cliff Front

Figs. 6 and 7 represent simultaneously the horizontal and vertical displacements at the cliff front. The global shape of the curves is the same for the different mesh sizes. But it is noticed that, as the mesh size is small, the curves take the same form (meshes 2m and 4m) and their values converge. However, at the foot of the cliff, the displacements are in the same range for all meshes.

Differences in values between the meshes of 2m and 4m have an average of 7cm for horizontal displacements and of 3.2cm for vertical displacements. These differences increase as the size increases, except at certain heights where horizontal displacements corresponding to the mesh of 10m approach those of the meshes of 2m and 4m.

The horizontal and vertical stresses on the cliff front

are simultaneously illustrated in Fig. 8 and Fig. 9. At 40m height to the crest, the stresses for the various meshes are almost equal, nearly null horizontally and linear vertically. Between 4m and 40m, their values vary. As the foot of the cliff is approached, where a high stress concentration is noticed, the values diverge

according to the mesh size. On the other hand, curves corresponding to meshes 2m and 4m converge better. The curve of mesh 10m follows well in the case of the horizontal stress but less better between 0 and 14m in the case of vertical stress.

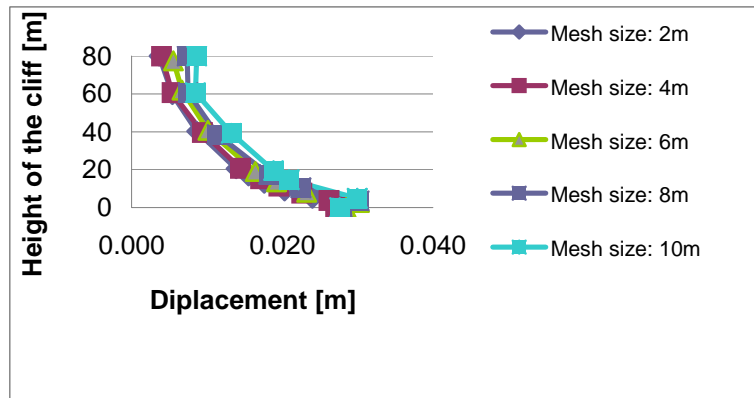


Figure (7): Vertical displacement at the cliff front in terms of cliff height

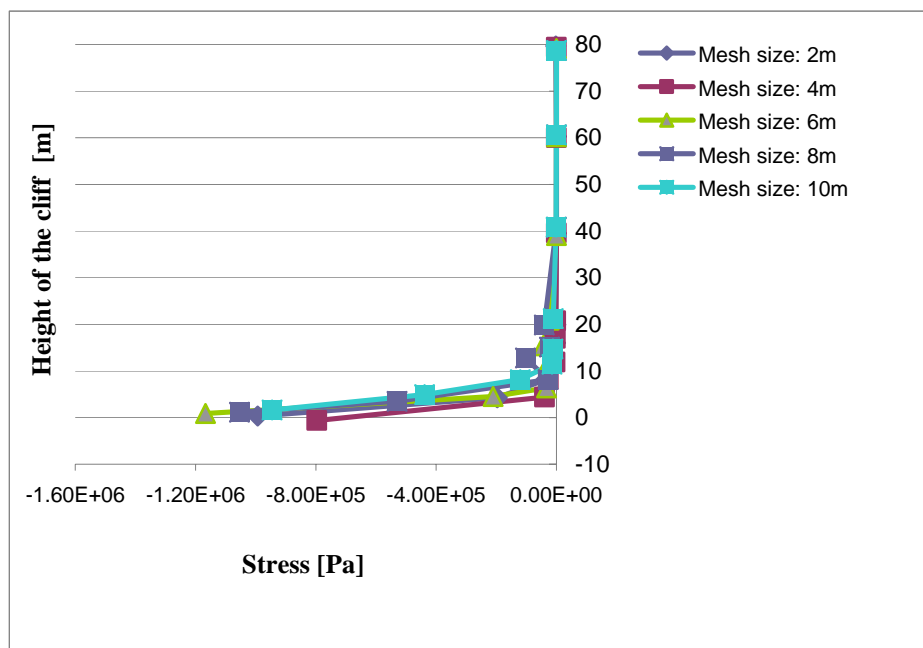


Figure (8): Horizontal stress at the cliff front in terms of cliff height

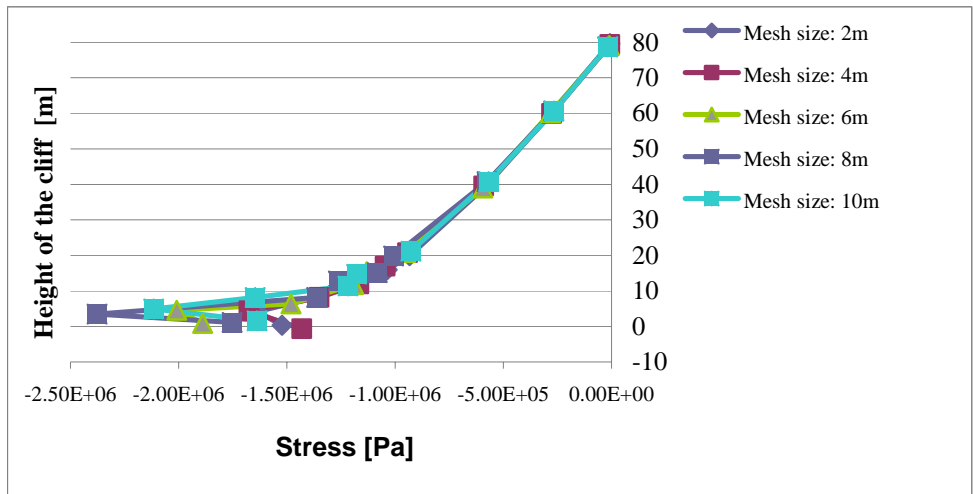


Figure (9): Vertical stress at the cliff front in terms of cliff height

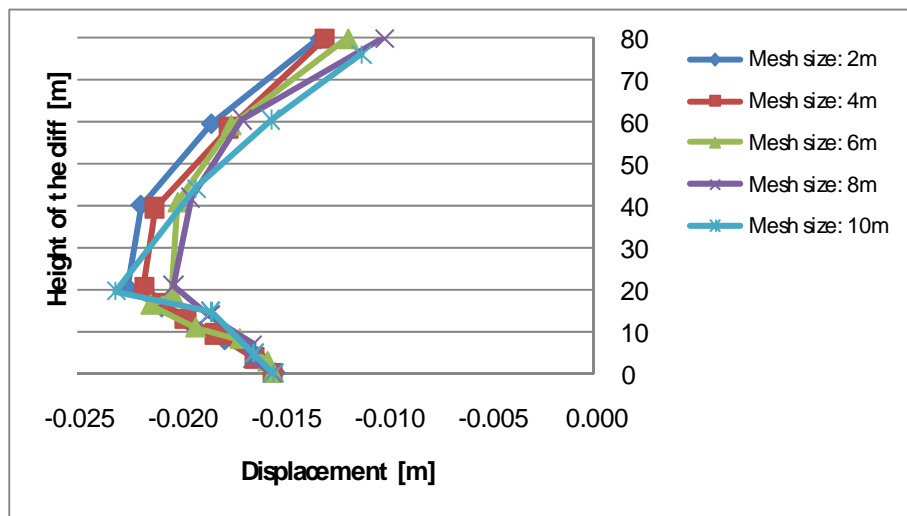


Figure (10): Horizontal displacement at 13 m from the cliff front in terms of cliff height

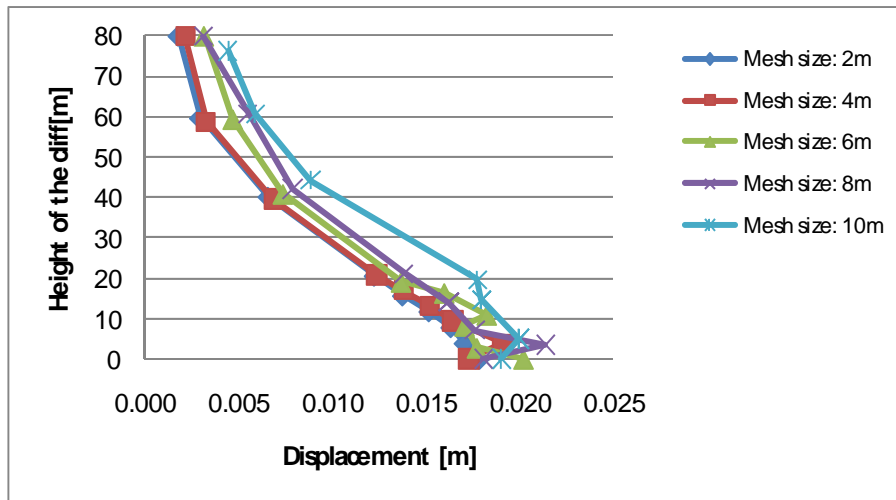


Figure (11): Horizontal displacement at 13m from the cliff front in terms of cliff height

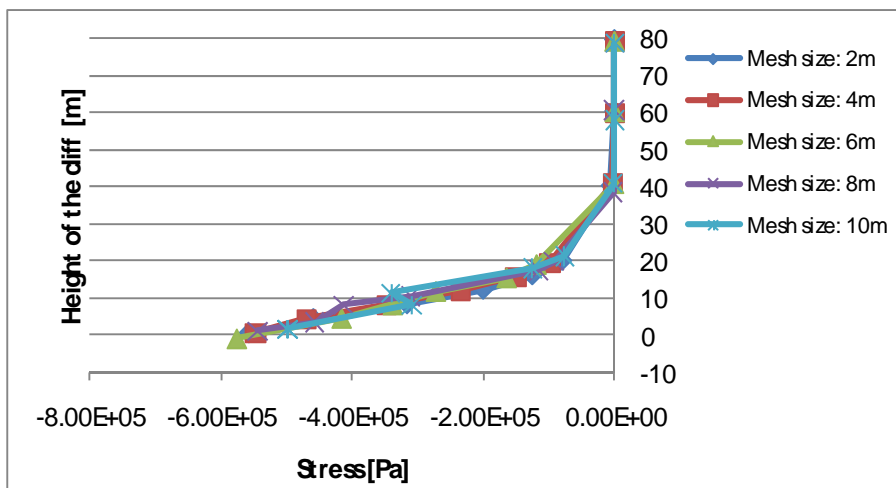


Figure (12): Horizontal stress at 13m from the cliff front in terms of cliff height

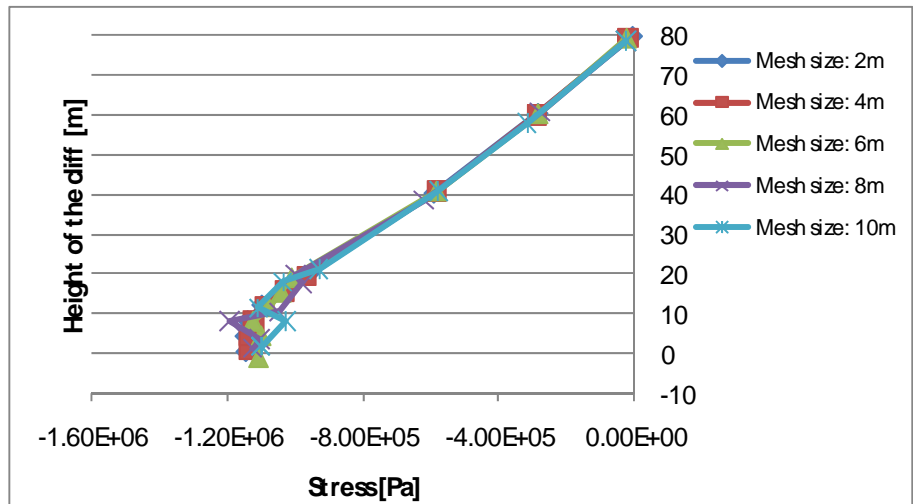


Figure (13): Vertical stress at 13m from the cliff front in terms of cliff height

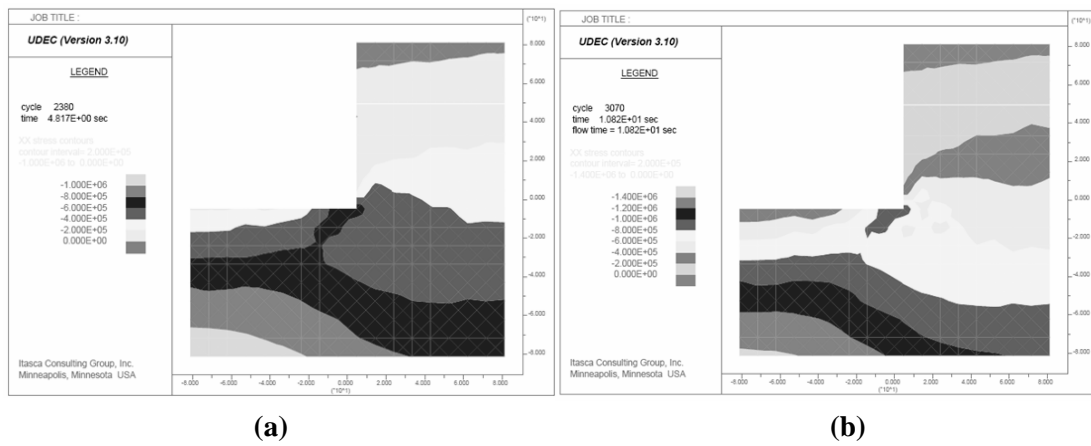


Figure (14): Horizontal stress state (Pa) of the cliff, a) dry, b) saturated

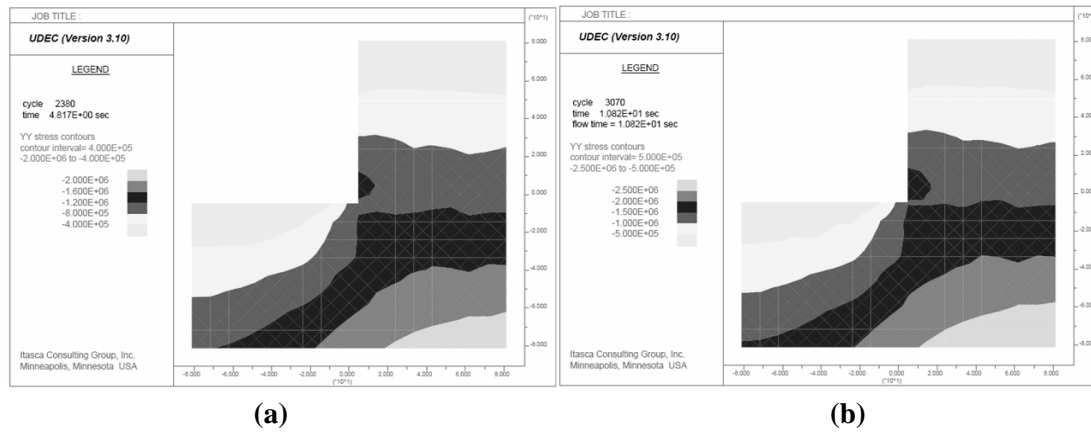


Figure (15): Vertical stress state (Pa) of the cliff, a) dry, b) saturated

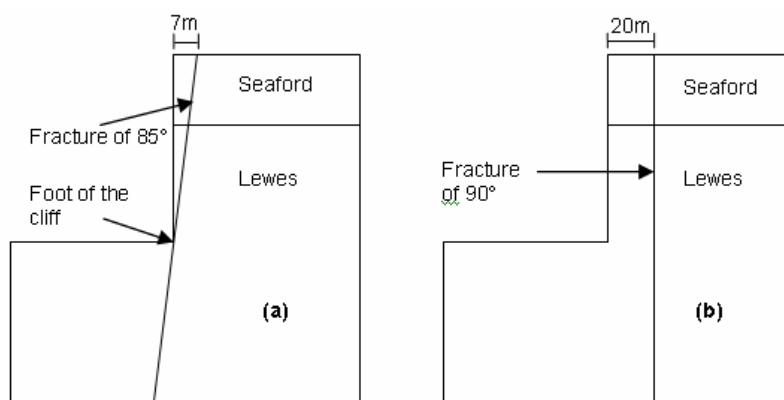


Figure (16): Cliff with fracture of: (a) 85°, (b) 90° with respect to horizontal level

Profile inside the Cliff

The values are taken at 13m inside the cliff compared to those at the cliff front. It is noticed that all the curves of displacements have the same shapes (Figures 10 and 11) compared to those of the profile of the cliff front, and these curves always correspond to the meshes of 2m and 4m which converge best.

In Figures 12 and 13, it is noticed that the curve which corresponds to the mesh of 6m starts to converge to those corresponding to the meshes 2m and 4m. It is obvious that as we move away from the sensitive zone, we are in less need of a fine mesh.

The mesh must thus be fine on the cliff front and coarse as we move away from this border, by respecting the ratio between dimensions of successive elements, which should not exceed 10% (Itasca, 1999).

APPLICATION TO THE CASE OF THE LARGE FLAGSTONES

Cliff with Two Layers without Fracture

The stress states according to X and Y are respectively illustrated in Figures 14 and 15 for a dry and a saturated cliff. It should be noted that the dry cliff is discretized by introducing the characteristics of material in the dry state; while the saturated cliff is discretized introducing, in addition to the characteristics

of material in the saturated state, the distribution of the hydrostatic pressure.

The stress distribution is similar in dry and saturated cases, nevertheless noticed variations appear in both cases. The low stress field is according to the horizontal one. The maximum value of stress in X direction equals -1MPa in the dry case and -1.4MPa in the saturated case; that is to say with a difference of 0.4MPa. For the case of stress in Y direction, the maximum value is -2MPa in the dry case and -2.5MPa in the saturated case; that is to say with a difference of 0.5MPa. In both cases, this difference in the stress is due to the presence of water. The cliff remains in equilibrium. It should be noted that the sign (-) indicates compression according to the convention of sign in UDEC.

Cliff with Two Layers and a Fracture

In this part of the study, the dip of the fracture is varied. We use a fracture having an angle of 85° with respect to the horizontal level passing by the foot of the cliff and a fracture with an angle of 90° with respect to the horizontal level at 20m from the cliff front (Fig. 16).

The state of plasticity for the cliff with a fracture of 85° and then with 90° is illustrated in Fig. 17. It can inform us about the type of possible failure. Fig. 17 indicates that during the computing process, a redistribution of stress took place; points passed from a

plastic state to an elastic state (similar to loading and unloading). With an orientation of 85° (Fig. 17a), the solid mass starts to show a traction in the cliff front with the crest, but the rupture is marked out within the fracture to a rupture by sliding plane (Fig.18a). On the other hand, in the fracture parallel to the cliff front (Fig. 17b), the area of traction extends from the top of the

cliff until the interface between the two layers (Seaford and Lewes) laterally limited, towards the interior of the solid mass, by the fracture, then it continues until a height of 20m above the foot of the cliff where it shows a corner of Coulomb, which can generate a rupture by sliding in this part, involving the effects of traction and tear off of the cliff top (Fig. 18b).

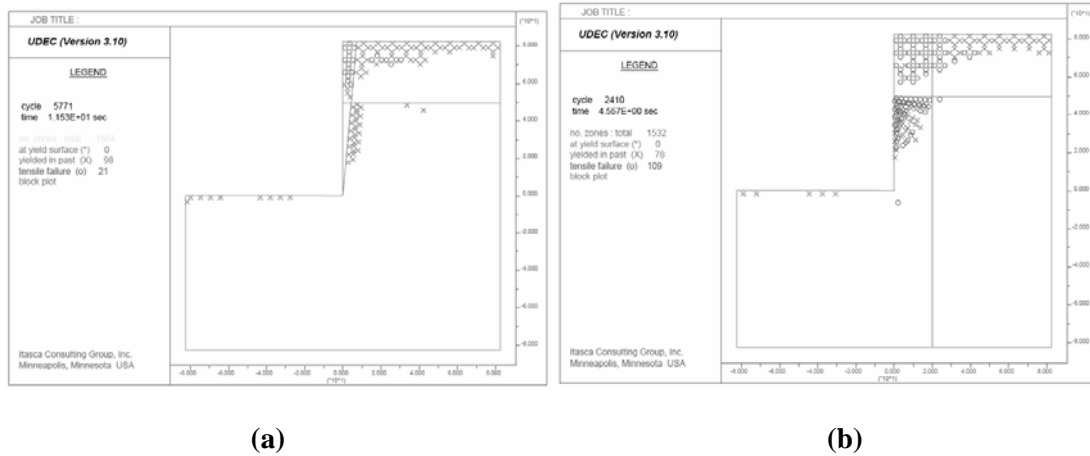


Figure (17): State of plasticity of the cliff with a fracture of: (a) 85°, (b) 90°

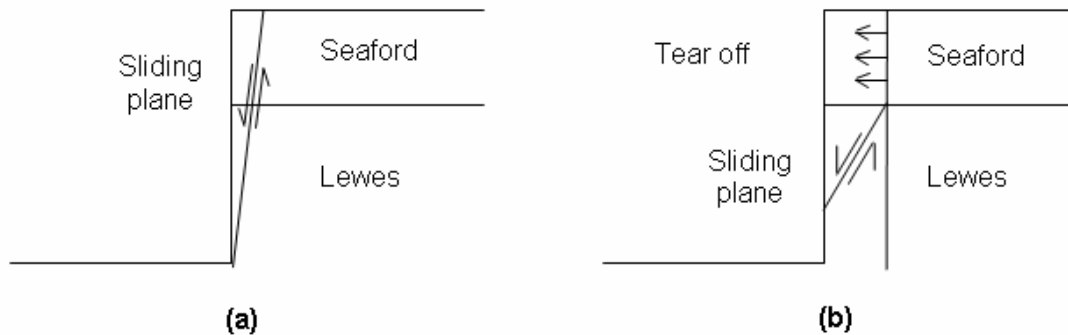


Figure (18): Illustration of sliding type with a fracture of a) 85° b) 90°

CONCLUSION

In this work, we give an idea about the model to be adopted to study the behavior of cliffs in terms of the mesh to be chosen for our structure, the boundary conditions to fix our profiles and the constitutive laws to

be used. In the case of cliff made up of two layers without fracture, the horizontal and vertical stress distribution is similar, whether in the dry or the saturated case. The cliff does not show instability and remains in equilibrium after calculation.

By introducing the fractures, the state of plasticity is

different depending on the orientation of the fracture. Two types of sliding appeared; the sliding plane in the presence of a fracture of 85° with respect to the horizontal level and a composed sliding plane on the lower part with tearing off of the cliff top in the presence of a fracture parallel to the cliff face.

The case of the cliff rupture with the presence of a fracture parallel to the cliff front corresponds well to the type of rupture observed in the field. Indeed, after crumbling a part of the cliff of large flagstones (July 2001, when nearly 60000 m³ of chalk were carried),

almost the same configuration illustrated in Fig. 18b is found. Observed scratches on the front of the cliff right on the Lewes layer let us deduce that there was a sliding plane on this part with a tearing off of the cliff top.

Results of the modeling of a cliff made up of two layers with a fracture parallel to the cliff front, by considering an elastoplastic law of Mohr-Coulomb type, agree well with the event that took place in the large flagstones, which can lead us to study other examples of cliff failure in the area of Haute Normandie by adopting the same steps.

REFERENCES

- Costa, S. 2000. Le recul des falaises du pays de Caux. *Bulletin d'information des Géologues du Bassin de Paris*, 37 (1): 31-34.
- Cundal, P.A. 1971. A computer model for simulating progressive large scale movements in blocky rock systems. In *Proceedings of the Symposium of the Int. Soc. Rock Mech.* (Nancy, 1971), 2-8.
- Dornbusch, U., Williams, R.B.G., Robinson, D.A. and Moses, C. 1996. Disappearing act: contribution of cliff erosion and *in situ* abrasion of flint to the shingle budget on the East Sussex coast. European rock coasts 2001 conference, Brighton, UK, 17-18 December 2001.
- Duperret, A., Genter, A., Mortimore, R.N., Delacourt, B. and De Pomerai, M. 2002. Coastal rock cliff erosion by collapse at Puys, France : the role of impervious marl seams within chalk of NW Europe. *Journal of Coastal Research*, 18 (1): 52-61.
- Duperret, A., Genter, A., Martinez, A. and Mortimore, R.N. 2004. Coastal chalk cliff instability in NW France : role of lithology, fracture pattern and rainfall. In : Mortimore, R.N. and Duperret, A. (Eds.), *Coastal Chalk Instability*, Engineering Geology Special Publication, vol. 20, Geological Society, London, 33-55.
- Duperret, A., Taibi, S., Mortimore, R.N. and Daigneault, 2005. Effect of groundwater and sea weathering cycles on the strength of chalk rock from unstable coastal cliffs of NW France. *Engineering Geology*, 78 (3-4): 321-343.
- Ferhah, M. 2002. Etude des caractéristiques mécaniques de la craie des falaises de Haute Normandie. Rapport de DESS Diagnostic et Réhabilitation des Architectures du Quotidien, année 2001-2002, LMPG, université du Havre, 63 pp.
- Indraratna, B. 2000. Single phase water flow through rock fractures. *Geotechnical and Geological Engineering*, 17: 211-240.
- Itasca. 1999. UDEC Version 3.1. Manual. Mineapolis: ICG.
- Lahousse, P. and Pierre, G. 2003. The retreat of chalk cliffs at cape Blanc-Nez (France): autopsy of an erosional crisis. *Journal of Coastal Research*, 19 (2): 431-440.
- Mas Ivars, D. 2006. Water inflow into excavations in fractured rock—a three-dimensional hydro-mechanical numerical study. *Int. J. Rock Mech. Min. Sci.*, 43, 705-725.
- Mortimore, R.N., Stone, K.J., Lawrence, J. and Duperret, A. 2004. Chalk physical properties and cliff instability. In: Mortimore, R.N. and Duperret, A. (Eds.), *Coastal Chalk Instability*, Engineering Geology, Special Publication, vol. 20, Geological Society, London, 75-88.